

## Carbon-13 and Proton NMR Spectroscopy of Four- and Five-Coordinate Cobalt(II) Porphyrins: Analysis of NMR Isotropic Shifts

ATAOLLAH SHIRAZI and HAROLD M. GOFF\*

Received January 18, 1982

Interpretation of carbon-13 NMR spectra for paramagnetic square-planar, low-spin cobalt(II) tetraphenylporphyrin derivatives confirms results of an earlier proton NMR study that attributed downfield phenyl isotropic shifts to the dipolar mechanism. Large contact contributions are apparent, however, for pyrrole and meso-carbon resonances. Signals for pyrrole and meso-carbon atoms are shifted upfield and downfield, respectively. This shift pattern is not expected for direct delocalization of unpaired spin from the  $\sigma$ -type  $d_{z^2}$  orbital but may be rationalized by a  $\pi$ -spin-polarization mechanism or by mixing of the  $^2E$  excited state as has been previously suggested by EPR measurements. Generation of the five-coordinate complex through attachment of a single pyridine ligand is associated with reduction of dipolar shift values and appearance of significant contact shift contributions for phenyl carbon atoms. Increased line broadening precluded observation of coordinated pyridine signals by carbon-13 or proton spectroscopy, but the far-downfield deuterium NMR signals of coordinated pyridine- $d_5$  are consistent with direct transfer of  $\sigma$ -type spin density from the  $d_{z^2}$  orbital.

### Introduction

Cobalt(II) porphyrins exist in the low-spin, square-planar configuration in noncoordinating solvents.<sup>1-4</sup> The cobalt(II) center has a high affinity for a single axial nitrogenous base such as pyridine and a lower affinity for binding of a second ligand.<sup>3-9</sup> Reversible binding of dioxygen to five-coordinate cobalt(II) porphyrins has been reviewed.<sup>10</sup> On the basis of numerous EPR studies it is known that the unpaired spin is localized in the axial  $d_{z^2}$  orbital ( $^2A_1$  state).<sup>6,7</sup> Significant magnetic anisotropy is apparent (with  $\chi_{\perp} > \chi_{\parallel}$ ) and is reduced by axial ligation, solvation, or porphyrin interactions with  $\pi$  donors.<sup>1,2,11-14</sup>

Proton NMR spectra of square-planar cobalt(II) porphyrins exhibit resonances that are significantly broadened and shifted up to 19 ppm with respect to diamagnetic metalloporphyrins.<sup>2,11</sup> These isotropic (paramagnetic) shifts have been attributed almost entirely to the dipolar (pseudocontact) shift term, which results as a consequence of metal ion magnetic anisotropy.<sup>2</sup> Only a small contact shift contribution might be anticipated, as the  $d_{z^2}$  orbital interacts weakly with the porphyrin  $\sigma$  system and is not of proper symmetry for  $\pi$ -orbital overlap.

The presumed dominant dipolar shift pattern for cobalt(II) porphyrins provides an example for evaluation of the parameters that may dictate carbon-13 NMR isotropic shifts. Conversely, carbon-13 measurements offer a means of validating interpretations made from proton NMR studies.<sup>2</sup>

Carbon-13 results reported here confirm the dipolar shift values for square-planar species but serve to demonstrate that much larger spin delocalization occurs in the macrocycle than was previously apparent in the less direct proton NMR measurements. Proton and carbon-13 measurements have also been extended to the five-coordinate pyridine and imidazole complexes.

### Experimental Section

Free base tetraphenylporphyrins (TPP)<sup>15</sup> and octaethylporphyrin (OEP)<sup>16</sup> were obtained by standard methods. A meso-carbon-13-labeled TPP was prepared with use of benzaldehyde (Merck) that was enriched 60 atom % at the carbonyl carbon atom.

Cobalt(II) porphyrins were prepared by a dimethylformamide or acetic acid reflux with cobalt(II) acetate and the free base porphyrin.<sup>17</sup> Products were purified by dry silica gel column chromatography with a methylene chloride eluent (containing 5% methanol for the *p*-methoxytetraphenylporphyrin species). Final crystalline products were obtained by simultaneous evaporation of methylene chloride and addition of pentane. Solid materials were vacuum-dried at 70 °C. Homogeneity of isolated materials was demonstrated by TLC on silica gel plates. Further characterization by visible-UV<sup>18,19</sup> and proton NMR<sup>2</sup> spectroscopy confirmed integrity of the cobalt(II) porphyrins. No precautions were necessary to prevent air oxidation during preparation or subsequent NMR spectral examination of cobalt(II) square-planar compounds. However, for the pyridine and imidazole ligation experiments, samples were prepared with use of degassed solvents in a Vacuum Atmospheres inter-atmosphere ( $N_2$ ) box.

Proton (90 MHz), carbon-13 (22.5 MHz), and deuterium (13.7 MHz) NMR measurements were performed on a JEOL FX-90Q spectrometer. Chemical shifts are reported with respect to internal  $Me_4Si$ , and downfield shifts are given a positive sign. Saturated cobalt(II) porphyrin solutions (0.015–0.05 M) in  $CDCl_3$  were required for natural-abundance carbon-13 work.

### Results

**Assignment of Carbon-13 Signals in Square-Planar Complexes.** The carbon-13 NMR spectrum of (TPP)Co is shown in Figure 1, and resonances for (TPP)Co and various phenyl-substituted analogues are listed in Table I at both 35 and 55 °C. In selected cases spectra were also recorded at 45 and 26 °C. Elevated temperatures were employed due to the low solubility of square-planar cobalt(II) porphyrins. Assignments of phenyl signals were based on the shift patterns observed for (TPP)Co, [TPP(*p*-CH<sub>3</sub>)]Co, [TPP(*m*-CH<sub>3</sub>)]Co, and [TPP-

- (1) La Mar, G. N.; Walker, F. A. In "The Porphyrins"; Dolphin, D., Ed.; Academic Press: New York, 1979; Vol. IV, pp 61–157.
- (2) La Mar, G. N.; Walker, F. A. *J. Am. Chem. Soc.* **1973**, *95*, 1790.
- (3) Walker, F. A. *J. Am. Chem. Soc.* **1973**, *95*, 1150.
- (4) Walker, F. A.; Beroiz, D.; Kadish, K. M. *J. Am. Chem. Soc.* **1976**, *98*, 3484.
- (5) Kadish, K. M.; Bottomley, L. A.; Beroiz, D. *Inorg. Chem.* **1978**, *17*, 1124.
- (6) Walker, F. A. *J. Am. Chem. Soc.* **1970**, *92*, 4235.
- (7) Walker, F. A. *J. Am. Chem. Soc.* **1973**, *95*, 1154.
- (8) Stynes, D. V.; Stynes, H. C.; Ibers, J. A.; James, B. R. *J. Am. Chem. Soc.* **1973**, *95*, 1142.
- (9) Stynes, D. V.; Stynes, H. C.; James, B. R.; Ibers, J. A. *J. Am. Chem. Soc.* **1973**, *95*, 1796.
- (10) Jones, R. D.; Summerville, D. A.; Basolo, F. *Chem. Rev.* **1979**, *79*, 139.
- (11) (a) Hill, H. A. O.; Mann, B. E.; Williams, R. J. P. *Chem. Commun.* **1967**, 906. (b) Hill, H. A. O.; Sadler, P. J.; Williams, R. J. P. *J. Chem. Soc., Dalton Trans.* **1973**, 1663. (c) Hill, H. A. O.; Sadler, P. J.; Williams, R. J. P.; Barry, C. D. *Ann. N.Y. Acad. Sci.* **1973**, *206*, 247. (d) Barry, C. D.; Hill, H. A. O.; Mann, B. E.; Sadler, P. J.; Williams, R. J. P. *J. Am. Chem. Soc.* **1973**, *95*, 4545. (e) Barry, C. D.; Hill, H. A. O.; Sadler, P. J.; Williams, R. J. P. *Proc. R. Soc. London, Ser. A* **1973**, *334*, 493. (f) Ford, L.; Hill, H. A. O.; Mann, B. E.; Sadler, P. J.; Williams, R. J. P. *Biochim. Biophys. Acta* **1976**, *430*, 413.
- (12) Fulton, G. P.; La Mar, G. N. *J. Am. Chem. Soc.* **1976**, *98*, 2119.
- (13) Walker, F. A. *J. Magn. Reson.* **1974**, *15*, 201.
- (14) Lin, W. C. In "The Porphyrins"; Dolphin, D., Ed.; Academic Press: New York, 1979; Vol. IV, pp 355–377.

- (15) Adler, A. D.; Longo, F. R.; Finarelli, J. D.; Goldmacher, J.; Assour, J.; Korsakoff, L. *J. Org. Chem.* **1967**, *32*, 476.
- (16) Wang, C.-B.; Chang, C. K. *Synthesis* **1979**, 548.
- (17) Adler, A. D.; Longo, F. R.; Varadi, V. *Inorg. Synth.* **1976**, *16*, 213.
- (18) Wayland, B. B.; Minkiewicz, J. V.; Abd-Elmageed, M. E. *J. Am. Chem. Soc.* **1974**, *96*, 2795.
- (19) Buchler, J. W.; Eikermann, G.; Puppe, L.; Rohbock, K.; Schneckhage, H. H.; Weck, D. *Justus Liebig's Ann. Chem.* **1971**, *745*, 135.

Table I. Carbon-13 NMR Spectra of Square-Planar Cobalt(II) Porphyrins<sup>a</sup>

C atom	(TPP)Co		[TPP( <i>p</i> -CH <sub>3</sub> )]Co		[TPP( <i>m</i> -CH <sub>3</sub> )]Co		[TPP( <i>p</i> -OCH <sub>3</sub> )]Co		(OEP)Co	
	35 °C	55 °C	35 °C	55 °C	35 °C	55 °C	35 °C	55 °C	35 °C	55 °C
ortho C	140.9	140.6	140.9	140.3	141.7	141.4	141.9	141.4		
meta C	130.2	130.3	131.3	131.0	138.0	137.7	116.0	115.8	184.2	177.7
					139.6	139.4				
para C	130.2	130.3	140.3	140.3	131.3	131.4	162.6	162.1		
phenyl C at meso	156.8	156.6	155.0	154.9	156.8	156.6	149.4	150.2		
meso C	204.5	200.1	<i>b</i>	198.5	<i>b</i>	198.5	203.7	<i>b</i>		
pyrrole α-C	60	<i>b</i>	<i>b</i>	<i>b</i>	<i>b</i>	67	<i>b</i>	<i>b</i>	70	<i>b</i>
pyrrole β-C	100.2	102.3	100.1	102.0	100.2	102.2	100.3	102.0	119.8	121.5
methyl C			23.5	23.3	23.4	23.4	57.1	57.0	21.3	22.0
methylene C									28.4	27.6

<sup>a</sup> CDCl<sub>3</sub> solvent, 0.02–0.03 M in cobalt(II) porphyrin. Signals are referenced to internal Me<sub>4</sub>Si. <sup>b</sup> Signal is under the solvent resonance or is not detected due to low solubility and poor sensitivity.

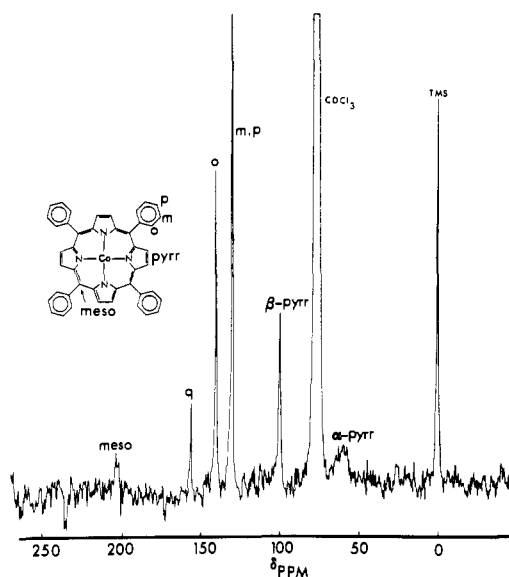


Figure 1. Carbon-13 NMR spectrum of (TPP)Co; CDCl<sub>3</sub> solvent, 35 °C.

(*p*-OCH<sub>3</sub>)]Co in proton-decoupled, coupled, and off-resonance broad-band-decoupled spectra. The quaternary phenyl carbon signal at 156.8 ppm is assigned by its appearance in this region for all TPP derivatives. The signal at 100.2 ppm represents the remaining proton-bearing carbon and must be assigned to the pyrrole β-carbon atom. Assignment of the meso-carbon signal at 204.5 ppm is made unequivocally through examination of the meso-carbon-13-enriched product. The remaining broad signal (near the chloroform solvent in Figure 1) is assigned to the pyrrole α-carbon atom.

The carbon-13 spectrum of (OEP)Co at 35 °C is shown in Figure 2, and chemical shift values are included in Table I. The signal at 184.2 ppm is that for a proton-bearing carbon atom. As expected, it is shifted upfield with respect to the quaternary meso-carbon resonance of (TPP)Co. Quaternary carbon signals at 119.8 and 70 ppm are reasonably assigned to the β- and α-carbon atoms, on the basis of the (TPP)Co spectrum. Ethyl group resonances in Figure 2 were readily assigned by a proton-coupled experiment.

Variable-temperature spectra are routinely recorded for paramagnetic metalloporphyrins to facilitate assignments and to check for Curie law behavior of isotropic shift values. Poor solubility of cobalt(II) porphyrins placed limitations on the accessible temperature range, and carbon-13 spectra were recorded only in the range from 26 to 55 °C. Earlier proton NMR results<sup>2,11</sup> showed Curie-type behavior at temperatures above 27 °C but serious deviations at lower temperatures due to specific solvation, aggregation, or magnetic anisotropy

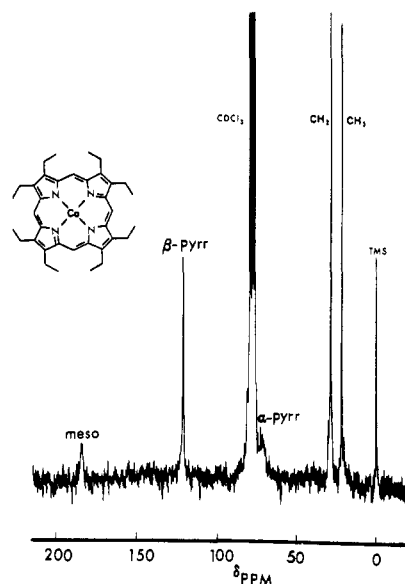


Figure 2. Carbon-13 NMR spectrum of (OEP)Co; CDCl<sub>3</sub> solvent, 35 °C.

Table II. Carbon-13 NMR Spectra for Addition of Trinitrobenzene to (TPP)Co<sup>a</sup>

C atom	[trinitrobenzene], M		
	0.0	0.08	0.20
ortho C	140.9	141.2	141.4
meta C	130.2	130.8	131.1
para C	130.2	130.8	131.1
phenyl C at meso	156.8	157.6	<i>b</i>
meso C	204.5	202.7	202.5
pyrrole α-C	60	65	<i>b</i>
pyrrole β-C	100.2	100.2	100.1
trinitrobenzene		123.2, 150.7	123.6, 149.5
ortho H	13.00	13.58	14.38

<sup>a</sup> CDCl<sub>3</sub> solvent, 0.02 M (TPP)Co, 35 °C, referenced to Me<sub>4</sub>Si. <sup>b</sup> Signal not located.

changes. Carbon-13 spectra at “high temperatures” also exhibit approximate Curie law behavior. For example, plots of isotropic shift vs.  $K^{-1}$  yield intercepts of 15 and -7 ppm for the meso-carbon signal of (TPP)Co and the pyrrole β-carbon signal of [TPP(*p*-OCH<sub>3</sub>)]Co, respectively.

**Trinitrobenzene Interactions with Square-Planar Complexes.** Fulton and La Mar<sup>12</sup> have used proton NMR to demonstrate formation of a specific π complex between [TPP(*p*-CH<sub>3</sub>)]Co and trinitrobenzene. Interaction of this π acceptor is associated with a downfield shift of up to 1.6 ppm for the ortho phenyl proton resonances, most likely as a consequence of increased metal ion magnetic anisotropy. Downfield shifts of this

Table III. Proton NMR Spectra of Five-Coordinate Cobalt(II) Complexes<sup>a</sup>

proton	(TPP)Co(py) <sup>b</sup>	[TPP( <i>p</i> -CH <sub>3</sub> )]- Co(py) <sup>c</sup>	[TPP( <i>m</i> -CH <sub>3</sub> )]- Co(py) <sup>c</sup>	(TPP)CoIm <sup>d</sup>	(TPP)Co- (1-CH <sub>3</sub> Im) <sup>d</sup>	(OEP)Co(py) <sup>c</sup>
pyrrole β-H	12.5	12.6	12.6	12.8	12.6	
ortho H	~8.5	~8.5	~8.5	~8.8	~8.8	
meta H	8.33	8.18	8.25	8.40	8.37	
para H	7.82		7.68	7.69	7.85	
-CH <sub>3</sub>		3.21	2.77			2.99
-CH <sub>2</sub>						3.6
meso H						9.3

<sup>a</sup> CDCl<sub>3</sub> solvent, 25 °C, Me<sub>4</sub>Si reference. Pyridine-*d*<sub>5</sub> and imidazole-*d*<sub>4</sub> were employed. <sup>b</sup> 0.01 M cobalt porphyrin, 0.2 M pyridine-*d*<sub>5</sub>. <sup>c</sup> 0.05 M cobalt porphyrin, 0.2 M pyridine-*d*<sub>5</sub>. <sup>d</sup> 0.01 M cobalt porphyrin, 0.01 M ligand.

magnitude were also observed for (TPP)Co at 35 °C (Table II) under the concentration conditions required for carbon-13 spectra. Table II summarizes carbon-13 NMR results with addition of two quantities of trinitrobenzene. Downfield carbon-13 NMR shifts for phenyl carbon atoms are somewhat smaller than those for respective protons. The meso-carbon signal surprisingly moves in an upfield direction upon trinitrobenzene interaction, and the pyrrole β-carbon signal is virtually unaffected. The pyrrole α-carbon signal is quite sensitive to trinitrobenzene complexation. Variable carbon-13 shift direction associated with trinitrobenzene complexation demonstrates that both dipolar and contact shift contributions are affected and that certain carbon-13 signals experience predominant contact shifts (vide infra).

**NMR of Five-Coordinate Complexes.** Although binding of nitrogenous bases has been described for cobalt(II) porphyrins,<sup>3-9</sup> corresponding NMR spectra have not been reported for the five-coordinate complexes. Addition of pyridine-*d*<sub>5</sub> to (TPP)Co yields the spectra shown in Figure 3. Peak assignment was made possible by rapid exchange between the four- and five-coordinate complexes, such that the titration of (TPP)Co with pyridine-*d*<sub>5</sub> yielded porphyrin signals that were mole-fraction weighted with respect to the two complexes. Thus, at 25 °C the pyrrole proton signal migrated from 15.73 ppm (the value for (TPP)Co) to 12.5 ppm as increasing amounts of pyridine were added. Phenyl assignments were further confirmed through examination of the *m*-methyl and *p*-methyl derivatives as listed in Table III. A similar titration was utilized for assignment of signals in (OEP)Co(py).

For both porphyrin structural types the proton NMR signals move toward the diamagnetic positions as an axial ligand is added. Unlike chemical shift values, however, line widths increase for all porphyrin positions. As an example, pyrrole proton line widths for four-coordinate vs. five-coordinate (TPP)Co are 116 and 290 Hz, respectively. Imidazole and 1-methylimidazole binding induces similar effects in the proton NMR spectrum (see Table III).

Binding of a single pyridine ligand to (TPP)Co is demonstrated through calculation of the equilibrium constant from spectra presented in Figure 3. With use of the pyrrole proton shift values, equilibrium constants of 345 and 333 M<sup>-1</sup> are calculated for parts b and c, respectively, of Figure 3 (the two values are not equivalent if bisligation is assumed). The average value of 340 M<sup>-1</sup> is to be compared with values of 794 M<sup>-1</sup> measured by electrochemical methods for pyridine binding to (TPP)Co in methylene chloride<sup>5</sup> and 485 M<sup>-1</sup> measured by visible-UV spectroscopy for pyridine binding to [TPP(*p*-OCH<sub>3</sub>)]Co in toluene.<sup>3</sup> Differences in these values may be due to concentration, aggregation, and solvent effects as well as the presence of supporting electrolyte for the electrochemical measurements. An equilibrium constant of 340 M<sup>-1</sup> dictates that >98% of the cobalt porphyrin is in the five-coordinate form at the 0.2 M pyridine concentrations typically employed for NMR work.

Ligation is also associated with changes in visible-UV spectra. Upon addition of 0.2 M pyridine to (TPP)Co the

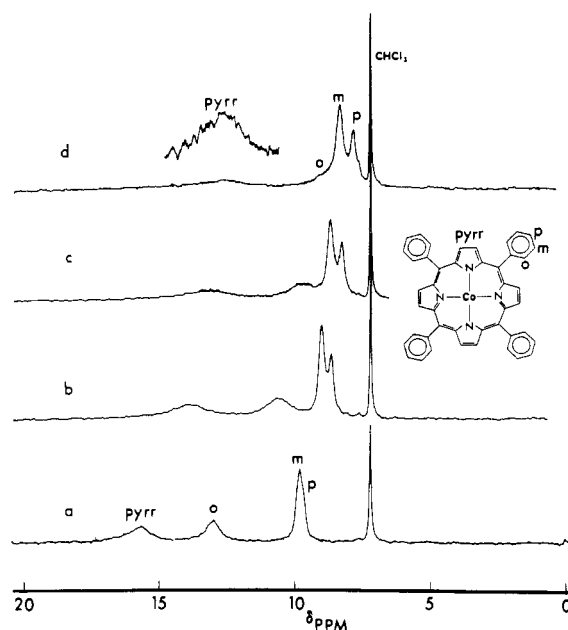


Figure 3. Proton NMR spectra for addition of pyridine-*d*<sub>5</sub> to (TPP)Co, with CDCl<sub>3</sub> solvent, 25 °C, and cobalt porphyrin concentration 0.01 M; pyridine-*d*<sub>5</sub> concentration: (a) 0.0 M; (b) 0.01 M; (c) 0.02 M; (d) 0.20 M.

absorption maxima originally at 408 and 538 nm are converted to values of 435, 549, and 585 (shoulder) nm. For (OEP)Co the absorption maxima change from 392, 520, and 552 nm to 420, 530, and 560 nm upon pyridine coordination.

Carbon-13 spectra reveal distinctive changes upon conversion to the five-coordinate species. Comparison of Figures 1 and 4 demonstrates that certain carbon-13 signals for the five-coordinate species are broadened beyond detection (for the particular experimental conditions employed here). Assignment of observable signals was possible on the basis of the migration of resonances for solutions containing increasing amounts of the five-coordinate complex. Assignment of the phenyl signals of (TPP)Co(py) was confirmed by examination of the *m*- and *p*-methyl analogues. The pyrrole α, meso, and quaternary phenyl carbon signals of (TPP)Co(py) were not detected due to extreme broadening. Use of meso-carbon-13-labeled material did, however, permit observation of the meso-carbon signal at 240 ppm. Carbon-13 chemical shift values are listed in Table IV.

Coordinated pyridine signals were not readily apparent in either the proton or the carbon-13 spectra, due to extreme line broadening and/or overlap with porphyrin resonances. Accordingly, experiments were performed with deuterium NMR of pyridine-*d*<sub>5</sub> complexes. Results are shown in Figure 5 for a solution 0.01 M in both pyridine-*d*<sub>5</sub> and (TPP)Co at 0 and 25 °C (Figure 5a,b), as well as for solutions containing excess pyridine (Figure 5c,d). Assignment of pyridine signals is tentative but follows from expected line widths on the basis of proximity to the metal center and areas of the three deu-

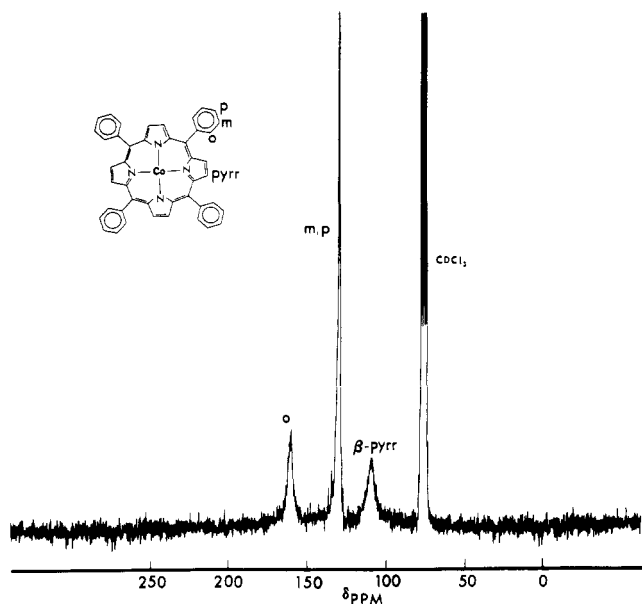


Figure 4. Carbon-13 NMR spectrum of (TPP)Co(py); CDCl<sub>3</sub> solvent, 35 °C, 0.05 M cobalt porphyrin, 0.20 M pyridine-d<sub>5</sub>.

Table IV. Carbon-13 NMR Spectra of Five-Coordinate Cobalt(II) Porphyrin Complexes<sup>a</sup>

C atom	(TPP)- Co(py)	[TPP( <i>p</i> -CH <sub>3</sub> )]- Co(py)	[TPP( <i>m</i> -CH <sub>3</sub> )]- Co(py)	(OEP)- Co(py)
ortho C	158.7	158.9	158.6	
meta C	129.1	129.8	128.9, 138.4	
para C	129.1	138.7	130.0	
phenyl C at meso	<i>b</i>	<i>b</i>	<i>b</i>	
meso C	240 <sup>c</sup>	<i>b</i>	<i>b</i>	<i>b</i>
pyrrole α-C	<i>b</i>	<i>b</i>	<i>b</i>	<i>b</i>
pyrrole β-C	109.4	109.4	109.8	123.7
methyl C		21.4	22.5	17.5
methylene C				29.0

<sup>a</sup> CDCl<sub>3</sub> solvent, 35 °C, Me<sub>4</sub>Si reference, cobalt(II) porphyrins 0.05 M, pyridine-d<sub>5</sub> 0.20 M. <sup>b</sup> Signal not located. <sup>c</sup> Meso-Carbon-labeled material was used; line width 1000 Hz.

terium signals. Deuterium signals are much more readily detected than corresponding proton signals when severe paramagnetic broadening is apparent. In the limit of dipolar relaxation, the line width is a function of the gyromagnetic ratio squared.<sup>20</sup> Thus, the proton line widths (in Hz) may be 42 times those of the deuterium nucleus. The titration results shown in Figure 5 serve to demonstrate that pyridine exchange is rapid on the deuterium NMR time scale. Chemical shift values at 25 °C represent a mole-fraction-weighted average of coordinated and free pyridine. On the basis of the equilibrium constant of 340 M<sup>-1</sup>, the pyridine signals in Figure 5b represent approximately 60% coordinated and 40% free pyridine. This permits calculation of the "limiting" chemical shift values for coordinated pyridine of 70 (α-deuterium) and 36 ppm (β-deuterium).

Variable-temperature NMR spectra of five-coordinate cobalt(II) porphyrin complexes are complicated by severe broadening of resonances at lower temperatures. This is evident for Figure 5a,b, in which case the α-deuterium signal nearly doubles in line width at 0 °C. Although this broadening could result from ligand-exchange dynamics, broadening of porphyrin proton signals is also evident with either stoichiometric or excess pyridine present and with excess imidazole or 1-methylimidazole present. Such broadening may well

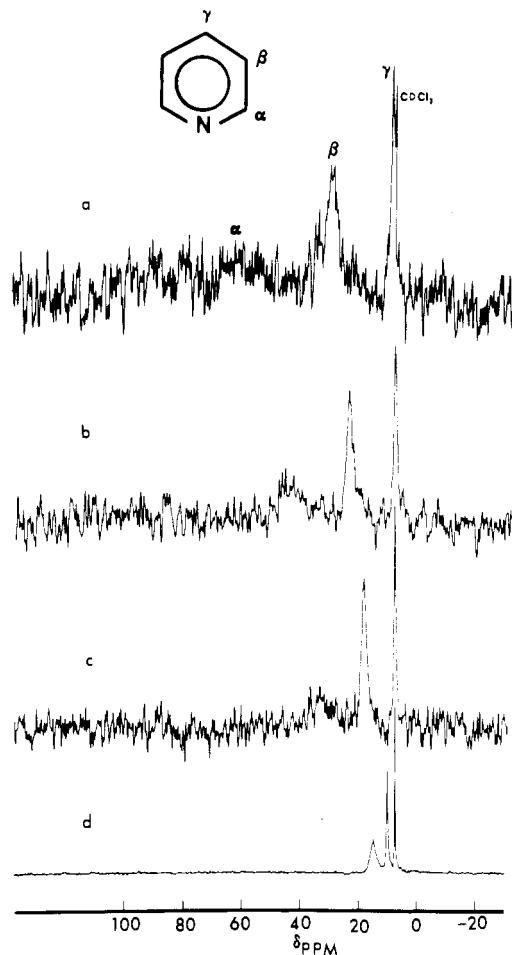


Figure 5. Deuterium NMR spectra for addition of pyridine-d<sub>5</sub> to (TPP)Co, with CHCl<sub>3</sub> solvent and 0.01 M cobalt porphyrin: (a) 0.01 M pyridine-d<sub>5</sub>, 0 °C; (b) 0.01 M pyridine-d<sub>5</sub>, 25 °C; (c) 0.02 M pyridine-d<sub>5</sub>, 25 °C; (d) 0.10 M pyridine-d<sub>5</sub>, 25 °C.

result from aggregation or ligand π-donor-π-acceptor complex formation. This complicating feature of variable-temperature measurements precluded quantitative interpretation of ligand-exchange dynamics.

### Discussion

**Determination of Magnetic Anisotropy.** For an NMR signal in a paramagnetic complex the isotropic shift is defined as the difference in ppm between this signal and that of the same nucleus in a diamagnetic reference compound. Corresponding cobalt(III) bis(1-methylimidazole) complexes, for which carbon-13 spectra have previously been reported,<sup>21</sup> have been chosen as diamagnetic references. Results would be essentially the same if the square-planar (TPP)Ni species was used as a diamagnetic reference, as carbon-13 signals are within 0.3 ppm of those for the cobalt(III) derivative.<sup>22</sup> Carbon-13 isotropic shift values are composed of three parts<sup>23</sup>

$$\frac{\Delta H_{\text{iso}}}{H} = \frac{\Delta H_{\text{con}}}{H} + \frac{\Delta H_{\text{dip}}^{\text{LC}}}{H} + \frac{\Delta H_{\text{dip}}^{\text{MC}}}{H}$$

where  $\Delta H_{\text{con}}/H$  is the contact contribution,  $\Delta H_{\text{dip}}^{\text{LC}}/H$  is a ligand-centered dipolar shift, and  $\Delta H_{\text{dip}}^{\text{MC}}/H$  is a metal-centered dipolar shift. For protons the  $\Delta H_{\text{dip}}^{\text{LC}}/H$  term is ex-

(20) Swift, T. J. In "NMR of Paramagnetic Molecules"; La Mar, G. N., Horrocks, W. D., Holm, R. H., Eds.; Academic Press: New York, 1973; Chapter 2.

(21) Goff, H. M. *J. Am. Chem. Soc.* **1981**, *103*, 3714.  
 (22) Due to low solubility (CDCl<sub>3</sub> solvent) only the proton-bearing carbon signals of (TPP)Ni were detected. Assignments are as follows: pyrrole β-C, 132.2; ortho C, 133.9; meta C, 127.0; para C, 127.9 ppm.  
 (23) McGarvey, B. R.; Kurland, R. J. In "NMR of Paramagnetic Molecules"; La Mar, G. N., Horrocks, W. D., Holm, R. H., Eds.; Academic Press: New York, 1973; Chapter 14.

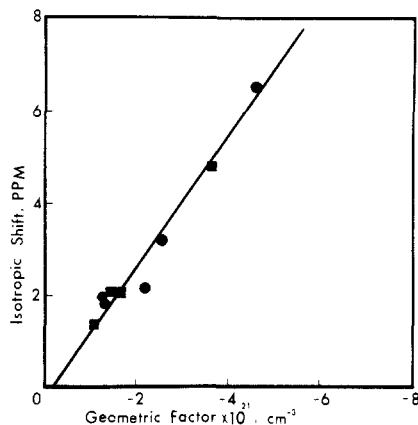


**Figure 6.** Plot of carbon-13 (●) and proton (■) isotropic shifts vs. geometric factors for square-planar [TPP(R)]Co species; CDCl<sub>3</sub> solvent, 55 °C.

pected to be negligible. The axial symmetry of synthetic porphyrins allows simplification of the metal-centered dipolar shift term to yield<sup>24</sup>

$$\frac{\Delta H_{\text{dip}}^{\text{MC}}}{H} = \frac{1}{3N}(\chi_{\parallel} - \chi_{\perp}) \frac{3 \cos^2 \theta - 1}{r^3}$$

where  $N$  is Avogadro's number and  $\chi$  values refer to molecular susceptibilities. The geometric factor,  $(3 \cos^2 \theta - 1)/r^3$ , defines the position of the observed nucleus with respect to the molecular axis and metal center. Separation of metal-centered dipolar shift values was possible in the earlier proton NMR study of square-planar cobalt(II) porphyrins by La Mar and Walker<sup>2</sup> on the basis of the assumed "insulation" of (TPP)Co phenyl protons from contact spin density. A rigorous test of this assumption is found in a plot of isotropic shift values vs. geometric factors (from the X-ray crystal structure<sup>25</sup>) for phenyl protons and carbon atoms as is shown in Figure 6. The collinearity of proton and carbon-13 data, as well as the near-zero intercept, provides reassurance that phenyl groups experience predominant metal-centered dipolar isotropic shifts.

The slope of the line in Figure 6 is equal to  $(\chi_{\parallel} - \chi_{\perp})/3N$ , and the value of  $\chi_{\parallel} - \chi_{\perp}$  is  $-2570 \times 10^{-6}$  cgsu. A solution magnetic moment of  $2.95 \mu_B$  measured by the Evans method<sup>26</sup> along with the relation

$$\bar{\chi} = \frac{1}{3}(\chi_{\parallel} + 2\chi_{\perp}) = 3300 \times 10^{-6} \text{ cgsu}$$

permits solution of  $\chi_{\parallel}$  and  $\chi_{\perp}$  to give  $\chi_{\parallel} = 1590 \times 10^{-6}$  cgsu and  $\chi_{\perp} = 4160 \times 10^{-6}$  cgsu. Calculation of  $g$ -tensor anisotropy from magnetic anisotropy demands a "pure" ground-state configuration with no mixing of excited states. Although this is a poor assumption for low-spin cobalt(II) (vide infra), the calculation is instructive for comparison with values obtained from proton NMR and EPR spectroscopy. The apparent  $g$ -tensor anisotropy value,  $g_{\parallel}^2 - g_{\perp}^2 = -9.0$ , is derived from the relations

$$\mu_i = 2.83(\chi_i T)^{1/2} \quad g_i = \mu_i[S(S+1)]^{-1/2}$$

where  $S = 1/2$ . The value of  $-9.0$  obtained here (at 55 °C) from combined proton and carbon-13 measurements is to be compared with the earlier proton NMR value of  $-8.2$  (at 35 °C)<sup>2</sup> and EPR values of  $-1.8$  and  $-7.8$  taken respectively at 77 K in a CHCl<sub>3</sub>/CH<sub>2</sub>Cl<sub>2</sub> glass and as a polycrystalline solid diluted with the metal-free porphyrin.<sup>26</sup> The seemingly major role of solvation is apparent in the frozen-glass EPR spectrum,

**Table V.** Separation of Carbon-13 NMR Isotropic Shift Terms for Square-Planar Cobalt(II) Porphyrins<sup>a</sup>

C atom	$10^{21} \times (3 \cos^2 \theta - 1)/r^3$	$\Delta H_{\text{iso}}/H$	$\Delta H_{\text{dip}}^{\text{MC}}/H$	$\frac{\Delta H_{\text{con}}/H + \Delta H_{\text{dip}}^{\text{LC}}/H}{H}$
ortho C <sup>b</sup>	-4.61	+6.5	+6.3	~0
meta C <sup>b</sup>	-2.55	+3.2	+3.3	~0
para C <sup>b</sup>	-2.20	+2.1	+2.8	~0
<i>m</i> -CH <sub>3</sub> <sup>c</sup>	-1.32	+1.8	+1.6	~0
<i>p</i> -CH <sub>3</sub> <sup>d</sup>	-1.28	+1.9	+1.5	~0
phenyl C at meso <sup>b</sup>	-8.4	+16.1	+11.6	+4.5
meso C	-25	+80 <sup>b</sup> +81 <sup>e</sup>	+35	+45 <sup>b</sup> +46 <sup>e</sup>
pyrrole α-C	-36	~-73 <sup>b</sup> ~-71 <sup>e</sup>	+51	~-124 <sup>b</sup> ~-122 <sup>e</sup>
pyrrole β-C	-13.0	-32 <sup>b</sup> -20 <sup>e</sup>	+18	-50 <sup>b</sup> -40 <sup>e</sup>
ethyl CH <sub>2</sub> <sup>e</sup>	-5.6	+7.3	+7.7	~0
ethyl CH <sub>3</sub> <sup>e</sup>	-3.0	+4.1	+4.0	~0

<sup>a</sup> CDCl<sub>3</sub> solvent, 55 °C. Cobalt(III) bis(imidazole) complexes were used as diamagnetic references. <sup>b</sup> For (TPP)Co. <sup>c</sup> For [TPP(*m*-CH<sub>3</sub>)]Co. <sup>d</sup> For [TPP(*p*-CH<sub>3</sub>)]Co. <sup>e</sup> For (OEP)Co.

whereas the "unsolvated" polycrystalline EPR magnetic anisotropy approximates that for (TPP)Co solutions at ambient temperature (as measured by NMR).

Five-coordinate complexes are not amenable to the analysis presented above, as significant contact shifts are apparent for phenyl carbon atoms of (TPP)Co(py). In this regard one should note the large downfield shift for the ortho phenyl carbon resonance in Figure 4 vs. the virtually unshifted meta and para phenyl carbon signals. Phenyl protons are better "insulated" from contact spin density, and a reasonable correlation can be made between isotropic shifts and geometric factors. However, given the significant phenyl carbon contact shifts, it would be presumptive to discuss the magnetic anisotropy other than to comment that the  $\chi_{\parallel} - \chi_{\perp}$  value must be 20% or less of that observed for square-planar species.

**Separation of Isotropic Shift Terms for Square-Planar Species.** Having shown that phenyl carbon isotropic shifts for square-planar species are predominantly dipolar, it is a simple matter to obtain the metal-centered dipolar shift for any atom of (TPP)Co by calculating the geometric factor and applying the linear function shown in Figure 6. Values are listed in Table V both for (TPP)Co derivatives and for (OEP)Co. The calculated metal-centered dipolar shift is subtracted from the isotropic shift to obtain the sum of contact and ligand-centered dipolar shift values.

The significant upfield of pyrrole α- and β-carbon  $\Delta H_{\text{con}}/H + \Delta H_{\text{dip}}^{\text{LC}}/H$  values is surprising in view of the assumed  $d_{xy}^2$ ,  $d_{xz}^2$ ,  $d_{yz}^2$ ,  $d_{z^2}^1$  electronic structure of cobalt(II) porphyrins. Thus, the half-filled  $d_{z^2}$  orbital is expected to interact (weakly) with the  $\sigma$ -type MO's to induce positive spin density and consequent downfield carbon contact shifts. Half-occupation of the  $d_{x^2-y^2}$  orbital as suggested by high-resolution X-ray diffraction data<sup>25</sup> is unreasonable (in solution), as the strongly interacting  $d_{x^2-y^2}$  unpaired spin should induce downfield shifts on the order of 1000 ppm much as is the case for high-spin iron(III)<sup>27-29</sup> and high-spin iron(II)<sup>30</sup> porphyrins.

Upfield shifts for pyrrole α- and β-carbon atoms are not readily explained by a  $\sigma$ -based spin-delocalization mechanism but are reminiscent of  $\pi$ -type delocalization.<sup>21</sup> This behavior

- (24) Horrocks, W. D. In "NMR of Paramagnetic Molecules"; La Mar, G. N., Horrocks, W. D., Holm, R. H., Eds.; Academic Press: New York, 1973; Chapter 4.  
 (25) Stevens, E. D. *J. Am. Chem. Soc.* **1981**, *103*, 5087.  
 (26) Evans, D. T. *J. Chem. Soc.* **1959**, 2003.

- (27) (a) Phillippi, M. A.; Goff, H. M. *J. Chem. Soc., Chem. Commun.* **1980**, 455. (b) Phillippi, M. A.; Baenziger, N.; Goff, H. M. *Inorg. Chem.* **1981**, *20*, 3904.  
 (28) Mispelner, J.; Momenteau, M.; Lhoste, J.-M. *J. Chem. Soc., Dalton Trans* **1981**, 1729.  
 (29) Goff, H. M.; Shimomura, E. T.; Phillippi, M. A., submitted for publication.  
 (30) Shirazi, A.; Leum, E.; Goff, H. M. *Inorg. Chem.*, in press.

may be rationalized by the previously characterized mixing of excited states with the ground state and/or by a spin-polarization mechanism. In particular, EPR spectra of square-planar cobalt(II) porphyrins are simulated only by including strong mixing of an excited  ${}^2E$  state,<sup>13,31</sup> as well as quartet states  ${}^4E$ ,  ${}^4A_2$ , and  ${}^4B_2$ .<sup>14,32</sup> Effective unpaired spin in the e-orbital set ( $d_{xz}$ ,  $d_{yz}$ ) for the  ${}^2E$ ,  ${}^4E$ , and  ${}^4B_2$  states is thus expected to give a shift pattern much as that for low-spin iron(III) porphyrins.<sup>21</sup> This is indeed the case for  $\alpha$ - and  $\beta$ -carbon resonances of (TPP)Co, which yield values of  $\Delta H_{\text{con}}/H + \Delta H_{\text{dip}}^{\text{LC}}/H$  of the same sign and essentially twice the magnitude as those for low-spin iron(III).<sup>21</sup> This direct comparison is complicated, however, by the fact that meso-carbon  $\Delta H_{\text{con}}/H + \Delta H_{\text{dip}}^{\text{LC}}/H$  values for square-planar cobalt(II) and low-spin iron(III) are of similar magnitude but of opposite sign. Utilization of the porphyrin  $4e(\pi^*)$  MO, which exhibits large amplitude at meso positions,<sup>1</sup> may serve to explain the downfield bias of the meso-carbon signal in square-planar cobalt(II) porphyrin complexes. Sizable spin density at the meso-carbon atom of the five-coordinate complex associated with appearance of the signal at 240 ppm implicates unpaired spin delocalization at this site through such a metal  $\rightarrow$  porphyrin  $\pi$ -MO charge-transfer mechanism. The carbon-13 spectra of other metal-TPP complexes for which this spin-delocalization pathway is operative also exhibit a far downfield ortho phenyl carbon resonance as a consequence of  $\pi$ - $\sigma$  spin polarization into the phenyl ring.<sup>27-29,33</sup> This mechanism induces a sizable downfield shift for the ortho phenyl carbon atom much as is observed in Figure 4.

An additional or perhaps alternate means of inducing  $\pi$ -type spin delocalization is found in the spin-polarization mechanism.<sup>34</sup> Thus,  $\sigma$ -spin density transferred from the  $d_{z^2}$  orbital to the pyrrole nitrogen atom may induce unpairing of spins in the pyrrole nitrogen  $\pi$  MO. Further polarization of the  $\pi$  system is expected to induce negative spin density (upfield shift) at the pyrrole  $\alpha$ -carbon atom and positive spin density (downfield shift) at pyrrole  $\beta$ - and meso-carbon atoms. Observed shifts follow this pattern for pyrrole  $\alpha$ - and meso-carbon atoms, but the pyrrole  $\beta$ -carbon signal is shifted upfield. In this regard it should be noted that the upfield ligand-centered dipolar shift term may dominate the  $\Delta H_{\text{con}}/H + \Delta H_{\text{dip}}^{\text{LC}}/H$  value as is the case for the pyrrole  $\beta$ -carbon resonance of low-spin iron(III) porphyrins.<sup>21</sup>

Appearance of  $\pi$  spin delocalization by either of the above mechanisms is not directly compatible with the relatively small pyrrole proton and meso-proton contact shift values of  $-2.4$  and  $+4.0$  ppm ( $35^\circ\text{C}$ )<sup>2</sup> for square-planar species. For an exclusive  $\pi$  spin-delocalization mechanism, proton contact shifts are directly related to the carbon  $\pi$  spin densities.<sup>34</sup> Thus, it is surprising that pyrrole proton contact shifts for low-spin iron(III)<sup>21</sup> and square-planar cobalt complexes are  $-19.5$  and  $-2.4$  ppm, whereas respective values of  $\Delta H_{\text{con}}/H + \Delta H_{\text{dip}}^{\text{LC}}/H$  are  $-25$  and  $-50$  ppm. Likewise, large carbon-13 shifts are observed for the ethyl groups of (OEP)Fe(Im)<sub>2</sub><sup>+</sup>,<sup>21</sup>

but shifts for (OEP)Co are attributed to only a small dipolar shift term (Table V). The only apparent explanation for these seeming discrepancies is found in assuming sizable  $\sigma$  spin delocalization in the macrocycle. The associated downfield shifts would tend to cancel the upfield  $\pi$ -contact contributions to yield rather small observed contact shifts.

**Comparison of NMR and EPR Results.** Changes in NMR spectra associated with axial ligation are consistent with the EPR analysis of various cobalt(II) porphyrins.<sup>32</sup> Binding of an axial ligand raises the energy of the  $d_{z^2}$  orbital and thus the energy of the  ${}^2E$  excited state, which has the configuration  $d_{xy}^2$ , ( $d_{xz}$ ,  $d_{yz}$ )<sup>3</sup>,  $d_{z^2}^2$ . A higher energy  ${}^2E$  state mixes less effectively with the  ${}^2A_1$  ground state to provide diminished unpaired spin density through the e-orbital set ( $d_{xz}$ ,  $d_{yz}$ ). This may account in part for the attenuated pyrrole  $\beta$ -carbon and proton shifts in five-coordinate complexes. Alternately it may be argued that ligation and expected doming of the porphyrin structure would perturb the spin-polarization contribution. Magnetic anisotropy, which induces the largely dipolar shifts of phenyl resonances, is also seemingly derived from the  ${}^2E$  state.<sup>32</sup> Diminished importance of the  ${}^2E$  contribution is thus apparent in that NMR dipolar shifts for the phenyl protons of five-coordinate complexes may be one-fifth those for the square-planar species. General broadening of porphyrin resonances in five-coordinate complexes also reflects the wider separation of the ground state and excited states. The electronic relaxation time,  $T_{1e}$ , for low-spin cobalt(II) is dependent on spin-orbit coupling of low-lying excited states. The longer  $T_{1e}$  value for five-coordinate complexes is thus associated with more efficient nuclear relaxation and broad NMR resonances.

The coordinated pyridine ligand interacts strongly with the unpaired spin in the  $d_{z^2}$  orbital. This is evident in the sizable downfield shift values observed in deuterium NMR spectra. Attenuation of shift values around the pyridine ring is strongly suggestive of the  $\sigma$  spin-delocalization mechanism expected for the  $d_{z^2}$  orbital. Such five-coordinate complexes provide an adequate model for the ligation state of cobalt(II) porphyrins reconstituted into apohemoproteins. These substitutions have been considered as a means of probing the heme environment through the large dipolar NMR shifts expected for cobalt(II) porphyrins.<sup>1,11d</sup> The results presented here show that decreased dipolar shifts and increased NMR line widths are expected for the relevant five-coordinate complexes. These factors make an NMR shift study unattractive but at the same time add to the possibilities for NMR relaxation measurements. Although dipolar shifts are small for five-coordinate cobalt(II) complexes with axial symmetry, it is entirely possible that rhombic perturbations in the protein could enhance contributions to the "nonaxial" dipolar term.<sup>24</sup> Significant isotropic shifts might also be apparent in the NMR spectrum of cobalt porphyrin reconstituted hemoproteins due to the large contact shift contribution expected for the axial (histidine) ligand.

**Acknowledgment.** Support from NIH Grant GM 28831-02 is gratefully acknowledged.

**Registry No.** (TPP)Co, 14172-90-8; [TPP(*p*-CH<sub>3</sub>)]Co, 19414-65-4; [TPP(*m*-CH<sub>3</sub>)]Co, 82265-76-7; [TPP(*p*-OCH<sub>3</sub>)]Co, 28903-71-1; (OEP)Co, 17632-19-8; (TPP)Co(py), 29130-61-8; [TPP(*p*-CH<sub>3</sub>)]Co(py), 60470-23-7; [TPP(*m*-CH<sub>3</sub>)]Co(py), 82281-53-6; (TPP)Co(Im), 79898-39-8; (TPP)Co(1-CH<sub>3</sub>Im), 51321-46-1; (OEP)Co(py), 82265-77-8; trinitrobenzene, 99-35-4.

(31) Lau, P. W.; Lin, W. C. *J. Inorg. Nucl. Chem.* **1975**, *37*, 2389.

(32) Lin, W. C. *Inorg. Chem.* **1976**, *15*, 1114.

(33) Mispelter, J.; Mometeau, M.; Lhoste, J.-M. *J. Chem. Soc., Chem. Commun.* **1979**, 808.

(34) La Mar, G. N. In "NMR of Paramagnetic Molecules"; La Mar, G. N., Horrocks, W. D., Holm, R. H., Eds.; Academic Press: New York, 1973; Chapter 3.